

Bulk Motions of Spiral Galaxies in the $z = 0.03$ Volume

Yu.N.Kudrya¹, V.E.Karachentseva¹, I.D.Karachentsev², S.N.Mitronova² and W.K.Huchtmeier³

¹*Astronomical Observatory, Kiev National University, Observatorna ul., Kiev, 304053 Ukraine*

²*Special Astrophysical Observatory, Russian Academy of Sciences, Nizhnii Arkhyz, Karachai-Cherkessian Republic, 357147 Russia*

³*Max Planck Institut für Radioastronomie, Auf dem Hügel 69, D-53121 Bonn, Germany*

Abstract

We analyze the peculiar velocity field for 2400 flat spiral galaxies selected from an infrared sky survey (2MFGC). The distances to the galaxies have been determined from the Tully–Fisher relation in the photometric J band with a dispersion of $0.^m45$. The bulk motion of this sample relative to the cosmic microwave background (3K) frame has an amplitude of 199 ± 37 km s⁻¹ in the direction $l = 290^\circ \pm 11^\circ, b = +1^\circ \pm 9^\circ$. The amplitude of the dipole motion tends to decrease with distance in accordance with the expected convergence of bulk flows in the 3K frame. We believe that external massive attractors similar to the Shapley cluster concentration are responsible for $\sim 60\%$ of the local flow velocity in the $z = 0.03$ volume.

PACS numbers : N.98

DOI: 10.1134/S1063773706010014

Key words : galaxies, Tully–Fisher relation, large-scale motions.

1 INTRODUCTION

Studying the bulk flows as the deviations from uniform Hubble expansion produced by large-scale gravitational effects is of particular interest in testing various cosmological models (Peebles 1980). The peculiar velocity of a galaxy is a measure of these deviations; apart from the Hubble distance determination, an independent distance determination is required to determine this velocity. The Tully–Fisher (TF) relation (Tully and Fisher 1977) and the Faber–Jackson (FJ) relation (Faber and Jackson 1976) together with its improved version, the Fundamental Plane (FP) method, remain the main popular methods for determining the distances to spiral and elliptical galaxies, respectively. The accuracy of determining individual distances by these methods is $\sim 20\%$, and the distances at which they are applicable can reach several hundred Mpc. In recent years, more accurate distance determination methods where the absolute magnitudes of type-Ia supernovae (SN Ia) (Riess et al. 1997) or the surface-brightness fluctuations (SBF) of galaxies (Tonry et al. 2000) are the distance indicators have been developed. Distances of several hundred Mpc can be estimated from SN Ia to within 8% (unfortunately, the number of measured supernovae is small). Distances as large as several tens of Mpc can be estimated by the SBF method with an accuracy of 10–20%.

A huge body of observational data (see, e.g., Willick (2000) Courteau and Dekel (2001), Zaroubi (2002) and references therein) pertaining separately to E and S galaxies, field galaxies,

cluster members, etc. has been accumulated over 20 years of active studies of non-Hubble flows. The works of different groups also differ by the depth of the samples studied and the peculiarities of the sky distribution of galaxies. The magnitude of the velocity and the direction of the bulk motion can be determined by measuring the radial peculiar velocities of galaxies. For the standard Λ CDM model, the bulk velocity in the cosmic microwave background (3K) frame is expected to approach zero as the volume under consideration increases. Therefore, measuring the dipole component on various scales is needed to determine the volume in which the flow converges. At present, there is no contradiction between the velocities ($\sim 220 \text{ km s}^{-1}$) and the directions of the bulk motions of galaxies estimated by different authors on a scale of $\sim 60 \text{ Mpc}$. At this depth, the data for E and S galaxies, field galaxies, and clusters are in good agreement, within the error limits, irrespective of the distance determination method (see Table 1 in the review by Zaroubi (2002)).

Two groups of results have been obtained at distances of 100–150 Mpc. Using 522 spiral galaxies in Abell clusters, Dale et al. (1999) determined the magnitude of the bulk velocity, $V = 75 \pm 92 \text{ km s}^{-1}$, and the apex position, $l = 282^\circ$ and $b = 25^\circ$ ($r \simeq 150 \text{ Mpc}$), by the TF method. Using 85 SN Ia, Riess et al. (1997) derived the apex position, $l = 289^\circ$ and $b = -2^\circ$, at a magnitude of the velocity that differs only slightly from zero. The results obtained by Colless et al. (2001) using the FP method apply to distant E galaxies in clusters located at distances of $H_0 r = 6000 - 15000 \text{ km s}^{-1}$ (EFAR) toward Hercules–Corona Borealis and Perseus–Pisces–Cetus. The authors found the bulk velocity in the volumes studied to be consistent with the hypothesis about its zero value at a 5% significance level. The above results are in good agreement: on scales of 100–150 Mpc, the bulk velocity is 0–200 km s^{-1} and the apex positions coincide, within the error limits, and are close to the direction of the excess of point sources in the sky from the IRAS PSCz catalog (Saunders et al. 2000). It is important that the convergence of bulk flows in this group of results was obtained for different types of objects and using different distance determination methods.

The second group of results is characterized by a high magnitude of the bulk velocity and a significant spread in apex positions. Based on photometry for the brightest galaxies in clusters, Lauer and Postman (1994) determined the parameters of the motion relative to the 3K frame for 119 Abell clusters of galaxies with velocities up to $15\,000 \text{ km s}^{-1}$ (LP): $V = 689 \pm 178 \text{ km s}^{-1}$, $l = 343^\circ$, $b = 52^\circ \pm 23^\circ$. Willick (1999) found the parameters of the bulk motion for 15 Abell clusters of galaxies located at a distance of 120 Mpc, $V = 720 \pm 280 \text{ km s}^{-1}$, $l = 272^\circ$, $b = 10^\circ$ (using the TF method). Hudson et al. (2004) found the parameters of the bulk motion in the 3K frame for 56 Abell clusters (the SMAC sample) up to $H_0 r = 6300 \text{ km s}^{-1}$ with an effective sample depth of $H_0 r_e = 6300 \text{ km s}^{-1}$: $V = 687 \pm 203 \text{ km s}^{-1}$, $l = 260^\circ \pm 13^\circ$, $b = 0^\circ \pm 11^\circ$. The authors believe that, apart from the Shapley Concentration, even more distant attractors must provide such a high velocity. Hudson (2003) attempted to reconcile the conflicting data at depths from 6600 to $11\,000 \text{ km s}^{-1}$ by assuming that the sample sparseness and small size lead to large errors in the peculiar velocities. If the LP sample is excluded, then the results with high and low bulk velocities can be reconciled at a 2σ level. The sample that combines the SMAC survey with other surveys yields a bulk flow with a velocity of $350 \pm 80 \text{ km s}^{-1}$ toward $l = 288^\circ$, $b = 8^\circ$ (Hudson 2003).

What the converge scale is remains an open question until new observational data based on much more complete and homogeneous samples are obtained. There are advantages and disadvantages in using clusters of galaxies to study the bulk motions. The distance determination

for a cluster is based on averaging the distances to its individual members, which reduces the error. However, the number of measured galaxies in clusters is generally small. In addition, including the cluster field galaxies remains a possibility. The number of clusters measured by various authors ranges from 20 to 100. Even if the cluster samples are distributed more or less uniformly over the sky, they are very sparse due to the small size. The measurement errors of the peculiar velocities for field galaxies are fairly large and increase with distance and sample incompleteness. This shortcoming is compensated for by the possibility of increasing the sample to hundreds or even thousands of galaxies. The Mark III catalog (Dekel et al. 1999) is an example of combining several catalogs of peculiar velocities to determine the parameters of the bulk motion. This catalog includes ~ 3000 E and S galaxies located at $R < 60$ Mpc. The Mark III galaxies move relative to the 3K frame with a bulk velocity of $V = 370$ km s $^{-1}$ toward $l = 305^\circ$, $b = 14^\circ$. This velocity seems fairly high compared to V obtained for other samples located in the same volume. The authors believe that an uncertainty in the mutual calibration of the heterogeneous samples may be responsible for the discrepancy.

Thus, an extensive deep homogeneous sample of galaxies uniformly and densely distributed over the sky is needed for a more definite solution of the question regarding the convergence scale of bulk flows. The edge-on flat galaxy catalog, RFGC (Karachentsev et al. 1999), satisfies these conditions. The RFGC includes 4236 galaxies with optical angular diameters $a > 0.6'$ and apparent axial ratios $a/b > 7$. The RFGC is currently the most uniform all-sky catalog of edge-on late-type spiral galaxies. About 3000 objects in the catalog have fairly reliable J, H, K photometry in the 2MASS survey (Cutri and Skrutski 1998), and ~ 1200 objects have estimates of the radial velocities V_h and the hydrogen line widths W_{50} . We constructed the 2MASS–TF relations for a sample of 1141 galaxies and, after cleaning, determined the parameters of the bulk motion for galaxies with $V_{3K} < 12000$ km s $^{-1}$ using 921 galaxies: $V = 226 \pm 62$ km s $^{-1}$, $l = 295^\circ \pm 16^\circ$, and $b = -2^\circ \pm 13^\circ$ (Kudrya et al. 2003).

Supplementing the 2MASS–RFGC sample to study the bulk flows suggests performing new measurements of V_h and W_{50} for RFGC galaxies. In particular, this program has been implemented with the 100-m Effelsberg radio telescope by Huchtmeier et al. (2005) and Mitronova et al. (2005) since 2001. Compiling a deeper homogeneous sample of late spirals based on the 2MASS catalog (2MFGC) is a fundamentally different possibility (Mitronova et al. 2004).

2 THE 2MFGC CATALOG

The successful application of the infrared (IR) Tully–Fisher relation to RFGC flat galaxies to determine the parameters of the bulk motion (Karachentsev et al. 2002; Kudrya et al. 2003) was a justification for compiling the new 2MFGC catalog. The 2MASS survey is known to have a low sensitivity with respect to late-type galaxies (Jarrett 2000), since the periphery of the disks of spiral galaxies is unseen on isophotes fainter than $K_s = 20^m$.

Studying the near-IR properties of RFGC galaxies and comparing them with optical data allowed the selection criteria to be worked out when compiling the new flat galaxy catalog based on 2MASS. Thus, for example, comparison of the IR and optical diameters of RFGC galaxies showed that the 2MASS diameters are, on average, half the standard optical radii. For RFGC galaxies, the optical axial ratios a/b cover the range (7–21) with a median of 8.6, while the corresponding IR axial ratios lie within the range (1–10) with a median of 4.1 (Karachentsev

et al. 2002).

The principles of selecting galaxies for the new catalog from the original 2MASS–XSC catalog were described in detail by Mitronova et al. (2004). The main parameter in the selection was the apparent axial ratio given in the XSC (Extended Sources Catalog). The all-sky 2MFGC disk galaxy catalog (Mitronova et al. 2004) contains IR photometry and identifications in the LEDA and NED databases for 18020 objects with axial ratios $a/b \geq 3$ in the XSC–2MASS. Analysis of the distribution of galaxies in axial ratio in the new catalog yields a median value of $a/b = 4$, which is close to the median value of $a/b = 4.1$ for the RFGC galaxies identified in the XSC–2MASS. The two catalogs are similar in morphological composition and contain $\sim 80\%$ of the late-type spiral galaxies.

Below, we use the following photometric parameters from the 2MFGC: J_{fe} , the elliptical Kron magnitude; r_{fe} , the elliptical Kron radius (in arcseconds) in the K band; a/b , the axial ratio averaged over all J , H , and K bands; and IC, the concentration index (the ratio of the radii within which $3/4$ and $1/4$ of the light from the galaxy is concentrated).

3 A SAMPLE FOR DETERMINING THE PARAMETERS OF THE BULK MOTION

Compiling a sample of 2MFGC galaxies with estimates of the heliocentric radial velocity V_h , the HI line width W_{50} , W_{20} , or the maximum rotational velocity V_m are the subject of a separate paper. The radial velocities are known for 5536 of the 18 020 2MFGC galaxies, and estimates of W_{50} , W_{20} , or V_m are also available for 2765 objects. The widths W_{50} (N=2276) and W_{20} (N=1825) are represented most completely in the sample. Both W_{50} and W_{20} estimates are available for 1740 sample galaxies. Optical measurements of V_m are available for 445 galaxies; 32 of them also have W_{50} estimates. To choose the basic width, W_{50} or W_{20} , in determining the parameters of the bulk motion, we first constructed the standard twoparameter TF relations for both widths. We take the TF relation in the form

$$M = C_1 + C_2 \log W^c. \quad (1)$$

We calculate the absolute magnitude from the apparent magnitude J_{fe} in the standard way,

$$M = J_{fe} - 25 - 5 \log r, \quad (2)$$

by first estimating the photometric distance r [Mpc] using the post-Hubble relation

$$r = V_{3K}/H_0 \{1 - (q_0 - 1)V_{3K}/2c\}, \quad (3)$$

where the radial velocity V_{3K} in the CMB frame is calculated from the heliocentric radial velocities $V_h = cz$ using the parameters of the solar motion relative to the background from Kogut et al. (1993). We take the Hubble constant $H_0 = 75 \text{ km s}^{-1} \text{ Mpc}^{-1}$ and the deceleration parameter $q_0 = -0.55$ in accordance with the cold dark matter (CDM) cosmological model and the cosmological constant ($\Omega_m = 0.3$, $\Omega_\Lambda = 0.7$).

We correct the widths for the cosmological expansion,

$$W^c = W/(1 + z), \quad (4)$$

by abandoning the correction for turbulence, which was applied in our previous paper (Kudrya et al. 2003), since it turned out to have no effect on the bulk velocity parameters. We determine the coefficients of relation (1) by least squares with equal weights.

We applied mainly the same data cleaning technique that was used previously (Kudrya et al. 2003) by excluding galaxies with deviations of more than $3\sigma_{TF}$ in the TF diagram and with individual peculiar velocities in the 3K frame $V_{pec} > 3000 \text{ km s}^{-1}$. In contrast to our previous paper (Kudrya et al. (2003), we did not exclude distance galaxies ($V_{3K} > 18000 \text{ km s}^{-1}$, $H_0 r > 18000 \text{ km s}^{-1}$) since there were only a few such objects. After the cleaning, we obtained samples of $N = 1604$ galaxies with W_{20} and $N = 1972$ galaxies with W_{50} . The

Table 1: Parameters of the Tully–Fisher relation for various samples

N	Sample	σ_{TF}	C_1	C_2	σ_V
1	$W_{20}, N1825$	1.01	-5.42 ± 0.35	-6.46 ± 0.14	1925
2	$W_{50}, N2276$	0.97	-7.14 ± 0.28	-5.86 ± 0.11	1927
3	$W_{20}, N1604$	0.55	-1.14 ± 0.23	-8.15 ± 0.09	992
4	$W_{50}, N1972$	0.49	-2.10 ± 0.18	-7.86 ± 0.07	974
5	$W_{50} + V_m, N2684$	0.92	-6.80 ± 0.25	-6.01 ± 0.10	1921
6	$W_{50} + V_m, N2333$	0.49	-2.55 ± 0.17	-7.69 ± 0.07	1015
7	$W_{50} + V_m + W_{20}, N2765$	0.94	-7.11 ± 0.25	-5.88 ± 0.10	1930
8	$W_{50} + V_m + W_{20}, N = 2395$	0.49	-2.68 ± 0.17	-7.64 ± 0.07	1016

results of our calculations are presented in the first two rows of Table 1 for the complete samples of $N = 1825$ galaxies with W_{20} and $N = 2276$ galaxies with W_{50} and in the third and fourth rows for the cleaned samples.

In Table 1, σ_{TF} denotes the standard deviation (in magnitudes) in relation (1), C_1 and C_2 are the coefficients in (1), and σ_V is the standard deviation (in km s^{-1}) in peculiar velocity space. In both cases, the scatter in the TF diagram is seen to be smaller for the widths W_{50} . Therefore, we take W_{50} as the basic width and then successively add the data with V_m and W_{20} to the sample with known W_{50} .

To pass from V_m to W_{50} , we used the relation

$$W_{50} = 2V_m + (27.4 \pm 7.8), \quad (5)$$

derived from 32 galaxies with measured W_{50} and V_m . In this way, we enlarged the sample by 408 objects, thereby bringing it to $N = 2684$.

The calculated parameters of the TF relation for the complete $N = 2684$ sample and for the $N = 2333$ sample cleaned using the adopted technique are given in the fifth and sixth rows of Table 1. We see that adding the data with V_m slightly reduced the scatter in the TF relation for the uncleaned data and left the scatter for the cleaned data unchanged.

Our sample contains 1740 objects with measured W_{50} and W_{20} . The relation between these widths is shown in Fig. 1.

After excluding the 68 galaxies that deviate from the linear relation by more than 3σ , we obtain the relation

$$W_{50} = W_{20} - (19.8 \pm 0.5). \quad (6)$$

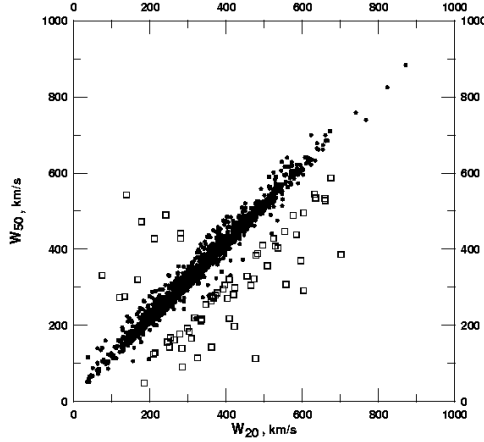


Figure 1: Relation between W_{50} and W_{20} . The squares mark 68 galaxies that deviate from the linear relation by more than 3σ .

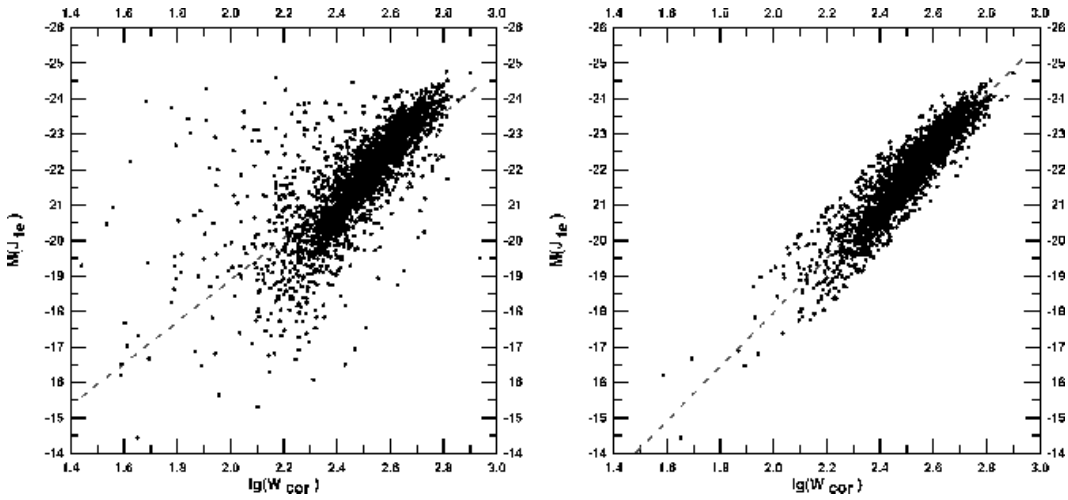


Figure 2: Tully–Fisher relations for the initial (a) and cleaned (b) samples.

The hypothesis that the coefficient of the linear correlation between the widths is equal to unity is confirmed by the Fisher test for an orthogonal regression. Adding the data with

W_{20} enlarged the sample by 81 galaxies. Parameters of the TF relation (1) for the complete, $N = 2765$, and cleaned, $N = 2395$, samples are given in the seventh and eighth rows of Table 1.

The Tully–Fisher relations for the initial and cleaned samples are shown in Fig. 2. The dashed lines in this figure correspond to the linear regression constructed by least squares.

We give Fig. 2a to illustrate the quality of the initial observational data. The region where most of the galaxies are concentrated is clearly seen, but an appreciable fraction of them (13%) exhibit a large scatter in the diagram. As we see from Fig. 1, this scatter is partly (by about 1/3) attributable to the low quality of the HI spectra. Comparison of Figs. 2a and 2b shows that our data cleaning criteria are efficient.

In the next section, we determine the parameters of the bulk motion for the cleaned $N = 2395$ sample.

Figure 3 presents the sky distribution of 2395 galaxies in Galactic coordinates. The galaxies with measured W_{50} ($N = 1977$), V_m ($N = 353$), and W_{20} ($N = 65$) are marked by filled circles, squares, and crosses, respectively. As we see, combining all of the data improves appreciably the uniformity of the sky distribution.

4 PARAMETERS OF THE BULK MOTION FOR 2MFGC GALAXIES

4.1 Basic Formulas and General Results

We used a simple two-parameter TF relation to compile our main sample of galaxies. To calculate the parameters of the bulk motion, we generalize relation (1) by including additional regressors. By an exhaustive search for various parameters of galaxies, we found that three regressors are most significant according to the Fisher test: the radius r_{fe} , the axial ratio a/b , and the concentration index IC. This linear relation is taken in the form

$$M = C_1 + C_2 \cdot \log W^c + C_3 \cdot \log r_{fe} + C_4 \cdot a/b + C_5 \cdot IC. \quad (7)$$

In this case, formulas (2)–(6) remain valid. We calculate the individual peculiar velocity in the post Hubble approximation,

$$V_{pec} = V_{3K} - H_0 r \{1 + (q_0 - 1)H_0 r / 2c\}. \quad (8)$$

We use the set of peculiar velocities to calculate the orthogonal components of the dipole bulk velocity V ,

$$V_{pec,i} = \vec{V} \cdot \vec{e}_i + \Delta V_i \quad (9)$$

by minimizing the sum of the squares of the “noise” peculiar velocity component V_i (i is the galaxy number in the sample). Here, $\vec{e}_i = (\cos l_i \cos b_i, \sin l_i \cos b_i, \sin b_i)$ is a unit vector of direction of galaxy i in a reference frame associated with the Galactic coordinates l and b . We calculated the errors in the magnitude of the bulk velocity V and the apex position l, b as follows. First, we determined the diagonal elements B_{VV} , B_{ll} , and B_{bb} of the covariance matrix \mathbf{B} in the basis $\{\vec{e}_V, \vec{e}_l, \vec{e}_b\}$ and then $\Delta V = (B_{VV})^{1/2}$, $\Delta l = \arctg\{(B_{ll})^{1/2}/V\}$, $\Delta b = \arctg\{(B_{bb})^{1/2}/V\}$.

The calculated bulk velocity parameters for the $N = 2395$ sample and for the samples of 2MFGC galaxies with the additional restrictions $V_{3K} < 8000 \text{ km s}^{-1}$ and $V_{3K} < 10000 \text{ km s}^{-1}$ are given in the first three rows of Table 2. Here, V_x, V_y, V_z denote the orthogonal components of the dipole bulk velocity, V is its magnitude (all in km s^{-1}), l and b are the Galactic coordinates of the apex, and F is the significance coefficient according to the Fisher test for the bulk velocity vector. Comparison of the first row in Table 2 and the eighth row in Table 1 shows that including the additional regressors reduces the scatter in the TF diagram by 6%.

To test the robustness of the results obtained and to illustrate the significance of the post-Hubble corrections in formulas (3) and (8), we calculated the parameters of the five-parameter regression and the bulk velocity by taking a linear Hubble law. The results for the $N = 2395$ sample are given in the fourth row of the table. We see that the apex position changed only slightly, while the magnitude of the bulk velocity increased by $\sim 5\%$. Our calculations for other

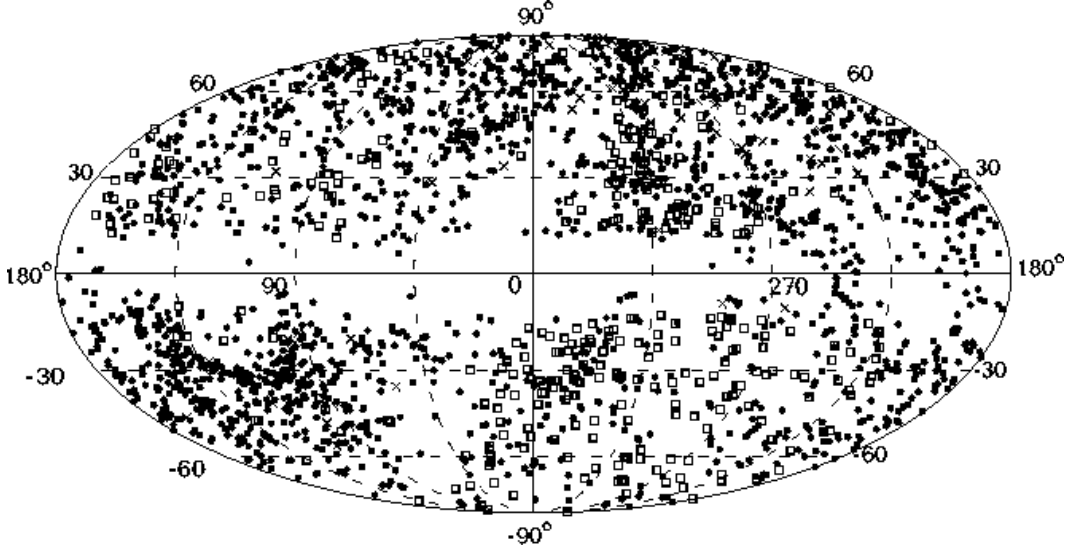


Figure 3: Distribution of 2395 2MFGC galaxies in Galactic coordinates. Galaxies with measured W_{50} , V_m , and W_{20} are denoted by filled circles, squares, and crosses, respectively.

samples also confirm that allowance for the relativistic redshift-distance relation slightly reduces the estimated magnitude of the bulk velocity.

We also checked how the sample cleaning based on the five-parameter regression (7) affected the parameters of the bulk motion. The galaxy selection criteria were the same as those for the two-parameter regression. The results of our calculations for the new $N = 2377$ sample are presented in the fifth row of Table 2. Comparison of the data in rows 5 and 1 shows a tendency for the magnitude of the velocity to decrease for a more rigorous sample cleaning. At the same

Table 2: Parameters of the dipole bulk velocity

N	Sample	σ_{TF}	σ_V	V_x	V_y	V_z	V	l	b	F
1	All, N2395	0.46	962	109 ± 37	-196 ± 37	-20 ± 31	225 ± 36	299 ± 10	-5 ± 8	13
2	$V_{3K} < 10000$, N2205	0.48	914	125 ± 37	-201 ± 37	-25 ± 30	238 ± 36	302 ± 9	-6 ± 7	15
3	$V_{3K} < 8000$, N1943	0.49	856	87 ± 37	-206 ± 37	-22 ± 30	225 ± 36	295 ± 10	-6 ± 8	14
4	LHL, N2395	0.46	970	110 ± 37	-206 ± 38	-28 ± 31	235 ± 37	298 ± 9	-7 ± 7	14
5	N2377	0.45	968	67 ± 37	-187 ± 38	2 ± 31	199 ± 37	290 ± 11	1 ± 9	10

time, the data in Table 2 indicate that the sought-for values of V , l , and b agree, within the error limits. Figure 4 presents the depth dependence of the magnitude of the bulk velocity (dots with bars, left vertical scale) and the sample size to a given depth (open diamonds, right vertical scale).

We see that the magnitude of the velocity decreases for distances from 3000 to 8000 km s^{-1} , as expected in the standard model for the formation of structures in the Universe with the cosmological constant and cold dark matter. The sample size increases roughly linearly to $V_{3K} = 8000$ – 10000 km s^{-1} and then is rapidly saturated. After 8000 km s^{-1} , the magnitude of the velocity (230–240 km s^{-1}) and the apex position (which is not given here) do not change, within the error limits. Thus, our results yield the magnitude and direction of the bulk velocity for 2MFGC galaxies to an effective depth of $\sim 10\,000 \text{ km s}^{-1}$.

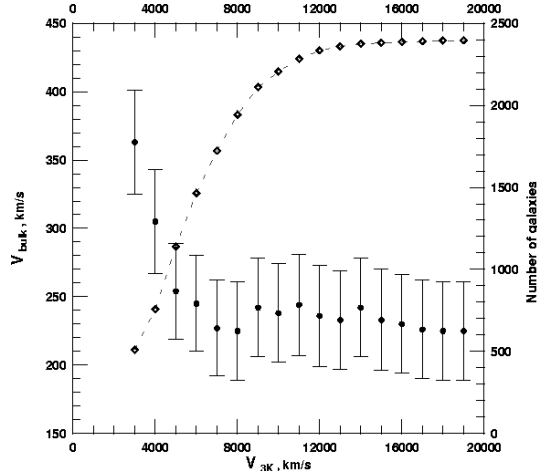


Figure 4: Magnitude of the bulk velocity (dots with bars, left vertical scale) versus depth and the sample size to a given depth (open diamonds, right vertical scale).

4.2 Parameters of the Bulk Motion for Spherical Shells

We also calculated the parameters of the bulk motion separately for four subsamples of the complete $N = 2395$ sample by breaking it down into shells: $0 < V_{3K} < 3000 \text{ km s}^{-1}$, S_1 ; $3000 < V_{3K} < 6000 \text{ km s}^{-1}$, S_2 ; $6000 < V_{3K} < 9000 \text{ km s}^{-1}$, S_3 ; and $9000 < V_{3K} < 20000 \text{ km s}^{-1}$, S_4 . The volumes of the first, second, third, and fourth subsamples include, respectively, the Local Supercluster ($l = 284^\circ$, $b = 74^\circ$), the Great Attractor (Hydra, $l = 270^\circ$, $b = 26^\circ$; Cen 30+45, $l = 302^\circ$, $b = 22^\circ$), the Coma supercluster ($l = 58^\circ$, $b = 88^\circ$), and the Shapley Concentration ($l = 312^\circ$, $b = 31^\circ$).

The sky distributions of galaxies in the shells in Galactic coordinates are shown in Fig. 5. The boundary of the shell (in km s^{-1}) and the number of galaxies in it are given in the upper left corner of each panel. The regions of enhanced density corresponding to well-known superclusters are clearly distinguished in the individual panels. Table 3 presents the calculated dipole bulk velocity. The parameters of the Tully–Fisher relation were determined for each shell separately. The content of the columns is the same as that in Table 3. As follows from these mutually independent data, the apex position and the bulk velocity amplitude in each shell remain approximately the same within $(1-2)\sigma$. The amplitude is at a minimum, $(157 \pm 45) \text{ km s}^{-1}$, in shell S_2 , where the Great Attractor is located. We see no evidence of the flow toward the Virgo cluster within the subsample S_1 with $V_{3K} < 3000 \text{ km s}^{-1}$; i.e., the entire volume of the Local Supercluster moves approximately in the same direction as the remaining objects of our sample.

4.3 Parameters of the Bulk Motion in the Frame of the Local Group

As we noted above, $\sim 13\%$ of the galaxies in the initial sample deviate significantly from the linear TF regression (see Fig. 2a). The low quality of the 2MASS photometry or the HI spectra for these galaxies is usually responsible for the deviations. Occasionally, the deviation from the TF relation is caused by the peculiar structure of a galaxy or the tidal perturbation from its close neighbors. We hoped to eliminate these cases by applying the three sigma rule

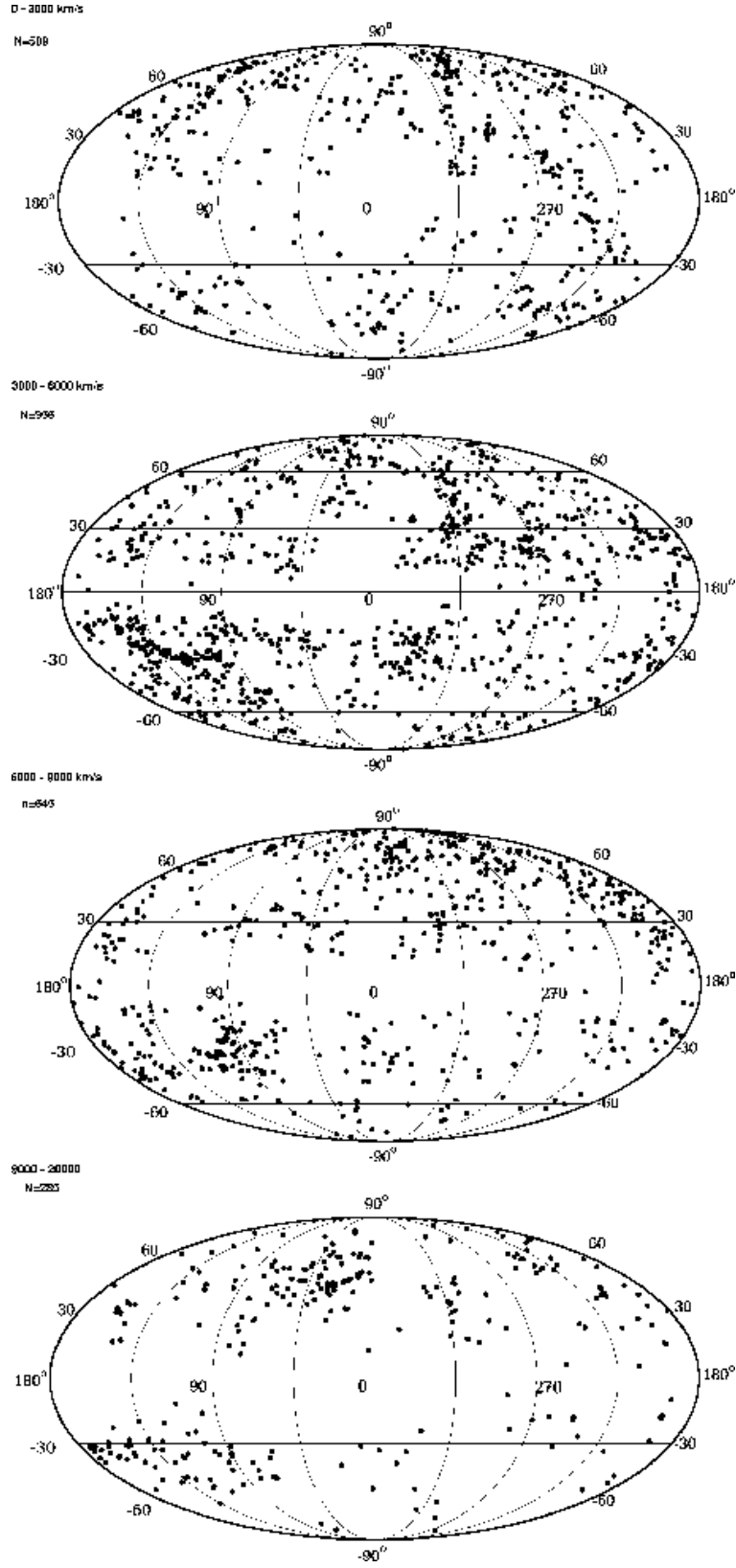


Figure 5: Sky distribution of galaxies in Galactic coordinates in the shells. The boundaries of the shell (in km s^{-1}) and the number of galaxies in it are indicated in the upper left corner of each panel.

and restricting the admissible absolute value of the peculiar velocity by the obvious physical limit $V_{pec} < 3000 \text{ km s}^{-1}$. As we see from relations (1)–(3) and (8), the adopted conditions for eliminating “bad” galaxies depend on the reference frame in which the distance and absolute magnitude of the galaxy are determined from its radial velocity. Therefore, in principle, the dipole parameters can contain a systematic error caused by the *a priori* choice of the 3K frame for estimating the distances to galaxies.

According to Kogut et al. (1993), the Sun moves relative to the 3K frame with a velocity of $V_{3K} = 369.5 \pm 3.0 \text{ km s}^{-1}$ in the direction $l = 264.4^\circ \pm 0.3^\circ$, $b = 48.4^\circ \pm 0.5^\circ$, while according

Table 3: Parameters of the dipole bulk velocity for galaxies in the spherical shells

N	Sample	σ_{TF}	σ_V	V_x	V_y	V_z	V	l	b	F
1	$S_1, N509$	0.57	438	236 ± 42	-276 ± 36	27 ± 27	364 ± 38	311 ± 6	4 ± 4	31
2	$S_2, N956$	0.37	738	38 ± 43	-145 ± 44	-47 ± 41	157 ± 45	285 ± 16	-17 ± 14	4.4
3	$S_3, N645$	0.30	1003	118 ± 73	-315 ± 83	-147 ± 61	367 ± 85	291 ± 11	-24 ± 9	6.4
4	$S_4, N285$	0.25	1187	157 ± 136	-287 ± 139	-75 ± 109	335 ± 143	299 ± 22	-13 ± 18	1.8

to Karachentsev and Makarov (1996), the Local Group centroid has a velocity of V_{3K} (LG) = $634 \pm 12 \text{ km s}^{-1}$ relative to the 3K frame in the direction $l = 269^\circ \pm 3^\circ$, $b = 28^\circ \pm 1^\circ$. The orthogonal components of this velocity V_x, V_y, V_z in the Galactic coordinate system are $(-8, -559, 298) \text{ km s}^{-1}$. To check the amplitude and direction of the bulk motion for the possible presence of a systematic error, we calculated the parameters of the dipole solution for 2MFGC galaxies from their velocities relative to the Local Group centroid and compared them with those obtained above in the 3K frame.

For $N = 2404$ galaxies that satisfied the three sigma rule and the condition $V_{pec} < 3000 \text{ km s}^{-1}$ in the LG frame, we obtained a standard deviation relative to the two-parameter TF relation of $\sigma_{TF} = 0.49^m$ or $\sigma_V = 986 \text{ km s}^{-1}$. The bulk motion of these galaxies in the LG frame has a velocity of $V = 372 \pm 33 \text{ km s}^{-1}$ in the direction $l = 76^\circ \pm 6^\circ$, $b = -40^\circ \pm 6^\circ$; the orthogonal components of this velocity are . Since

$$\vec{V}_{3K}(2MFGC) = \vec{V}_{LG}(2MFGC) + \vec{V}_{3K}(LG),$$

returning to the 3K frame, we obtain the orthogonal bulk velocity components $(+60, -284, +57)$ or the following new amplitude and direction of the bulk motion: $V = 296 \text{ km s}^{-1}$, $l = 282^\circ$, $b = 11^\circ$. Comparison with the previous data (see row 1 in Table 2) shows that the systematic difference in the parameters of the bulk motion due to different galaxy elimination procedures lies within 2σ of the random errors. However, it should be noted that the systematic difference in V_x, V_y, V_z is more significant in the close volumes S_1 and S_2 .

4.4 The Peculiar Velocity Field

The distribution of the peculiar velocities for 2MFGC galaxies defined by relations (7) and (8) is presented in Galactic coordinates in Fig. 6. Galaxies with positive and negative peculiar velocities are indicated by the open and filled circles, respectively. This discrete distribution was averaged by a Gaussian filter with a 20° window. Equal mean peculiar velocities are indicated by the lines at 50 km s^{-1} steps. The heavy line corresponds to a zero peculiar velocity; negative V_{pec} are indicated by the dashes.

As follows from these data, the peculiar velocity distribution of 2MFGC galaxies is asymmetric: the maximum positive isovelocity is $+350 \text{ km s}^{-1}$, while the maximum negative isovelocity is only 150 km s^{-1} . The V_{pec} distribution shows a distinct dipole pattern. The region of positive mean V_{pec} appears doubly connected, with the primary peak being approximately in the zone where the Hydra–Centaurus, Norma, A3627 clusters and the Shapley Concentration of clusters are located. The secondary positive peak with an amplitude of 150 km s^{-1} is identified with the Abell cluster A400 ($170^\circ, -45^\circ$) and A539 ($196^\circ, -18^\circ$). The region of negative mean peculiar velocities forms three broad shallow troughs with the coordinates of their centers ($120^\circ, +40^\circ$), ($80^\circ, -30^\circ$), ($200^\circ, +30^\circ$). The first two of them lie not far from the well-known Void in Bootes and the Local Void. In general, the relief of the crests and troughs in Fig. 6 agrees well with that obtained from a less representative sample ($N = 971$) of RFGC galaxies with 2MASS photometry (Kudrya et al. 2003). The reproducibility of general features in the V_{pec} distribution from two essentially independent observational samples gives hope that the distribution of the gravitational potential in the local Universe can be reconstructed from the available peculiar velocity map.

5 DISCUSSION AND CONCLUSIONS

To estimate the representativeness and quality of the galaxy sample used to determine the dipole parameters, we introduced the concept of goodness, $G = (N/100)^{1/2}/\sigma_{TF}$, where N is the number of galaxies in the sample, and TF is their dispersion (in magnitudes) in the TF diagram (Kudrya et al. 2003). Of course, apart from N and σ_{TF} , the quality of the sample is also characterized by the uniformity with which it covers the entire sky. However, allowance for the nonuniform distribution of galaxies over the sky requires more complex approaches. At present, there are only five samples whose goodness exceeds $G = 5$. They are all listed in Table 4 in order of increasing G . Columns 1, 2, and 3–5 give the galaxy type, its goodness G , and the dipole amplitude and direction in Galactic coordinates, respectively; the last column gives a reference to the data source.

As follows from these data, the sample of 2MFGC galaxies being discussed has the best goodness. The parameters of the 2MFGC dipole are in good agreement with their weighted mean values for all five samples: $V = 225 \pm 47 \text{ km s}^{-1}$, $l = 295^\circ \pm 3^\circ$, $b = +6^\circ \pm 5^\circ$. These amplitude and direction of the bulk motion can be currently taken as the standard ones for the bulk flow of galaxies relative to the CMB on a scale of $\sim 100 \text{ Mpc}$. It should be noted that this direction of the dipole is almost opposite to the direction of the rotational velocity of the Sun relative to the Galactic center, $V = 220 \text{ km s}^{-1}$, $l = 90^\circ$, $b = 0^\circ$. For this coincidental reason, the large-scale flow of galaxies had gone unnoticed until the 1980s.

Recall that we compiled and used catalogs of edge-on spiral galaxies to analyze the bulk motions of galaxies. The selection of such galaxies by their optical parameters (FGC) led to the following apex parameters: $V = 300 \pm 75 \text{ km s}^{-1}$, $l = 328^\circ \pm 20^\circ$, and $b = 78^\circ \pm 158^\circ$ (Karachentsev et al. 1993). An increase in the sample size in combination with the passage from optical to IR photometry yielded new apex parameters: $V = 199 \pm 61 \text{ km s}^{-1}$, $l = 301^\circ \pm 18^\circ$, and $b = -2^\circ \pm 15^\circ$ (Kudrya et al. 2003). Using the new 2MFGC catalog compiled from the 2MASS survey provided a more uniform distribution of galaxies over the sky. The amplitude and direction of the bulk flow calculated here, $V = 199 \pm 37 \text{ km s}^{-1}$, $l = 290^\circ \pm 11^\circ$, and

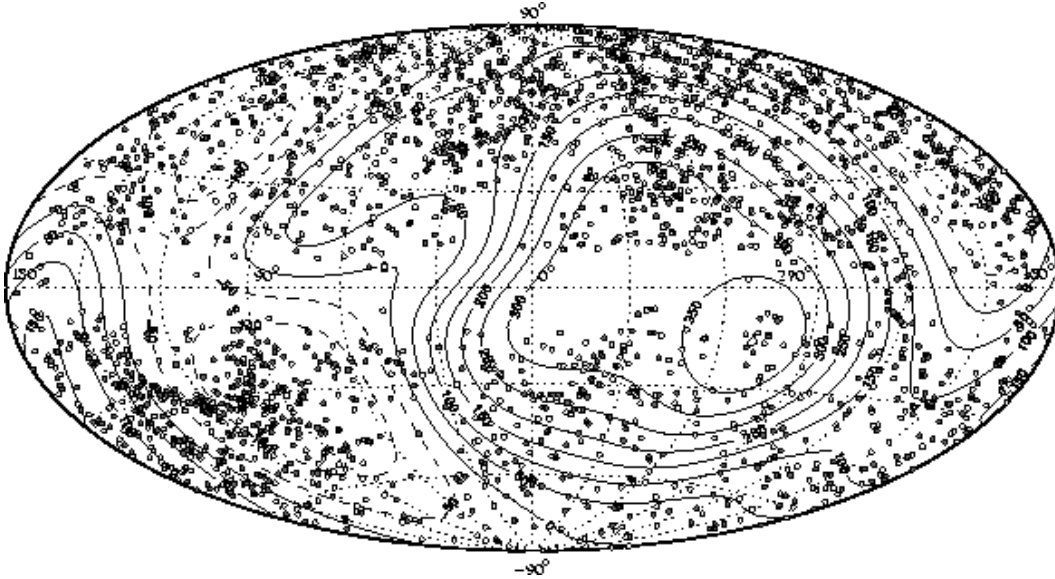


Figure 6: Peculiar velocity distribution for 2395 2MFGC galaxies in Galactic coordinates. Galaxies with positive and negative peculiar velocities are indicated by the open and filled circles, respectively. The velocities of the galaxies were averaged by a Gaussian filter with a 20 window. The lines of constant mean peculiar velocity are indicated at 50 km s^{-1} steps. The heavy line corresponds to a zero peculiar velocity; negative V_{pec} are indicated by the dashes.

$b = +1^\circ \pm 9^\circ$, are in satisfactory agreement with our previous dipole solutions (Karachentsev et al. 2000). Thus, our parameters of the local large-scale flow turned out to be stable with respect to the selection of galaxies by their optical or IR parameters, the use of the optical or IR luminosities in the TF diagram. The dipole parameters also change little if other regressors are included in the standard TF relation between absolute magnitude and 21-cm line width: the axial ratio, the surface brightness, the concentration index, and quadratic combinations of these regressors. The manner of eliminating galaxies by their peculiar velocity (in the 3K or LG frame) introduces a systematic errors within 2σ of the random errors.

Table 4: Goodness for various samples

Sample	G	V	l	b	Reference
Spirals in clusters	6.0	75	289	25	Dale et al. (1999)
SNIa	6.8	206	290	0	Radburn-Smith et al. (2004)
RFGC	7.4	199	301	-2	Kudrya et al. (2003)
Mark III	8.6	370	305	14	Dekel et al. (1999)
2MFGC	10.9	199	290	1	This paper
Mean	—	225	295	6	—

The apex of the bulk flow is located roughly in the same region as the centroids of IRAS sources ($l = 258^\circ, b = +30^\circ$), the centroid of 2MASS galaxies ($l = 278^\circ, b = +38^\circ$), and the concentrations of rich Shapley clusters ($l = 315^\circ, b = +30^\circ$). If judged by the pattern of decrease in the flow amplitude in Fig. 4 with linear scale of the Local Volume, then objects

(attractors) located farther than 50 Mpc could be responsible for $\sim 60\%$ of the amplitude of the observed bulk motion of 2MFGC galaxies.

ACKNOWLEDGMENTS. We wish to thank D. Makarov for help in preparing Fig. 6. Here, we used data from the 2MASS survey, which is a joint project of the Massachusetts University and the Infrared Data Processing and Analysis Center sponsored by NASA and NSF. We used the LEDA database (<http://leda.univ-lyon1.fr>). This study was supported by the DFG–RFBR grant 436RUS 113/701/0–1.

References

- [1] M. Colless, R. P. Saglia, D. Burstein, et al., *Mon. Not. R. Astron. Soc.* 321, 277 (2001).
- [2] S. Courteau and A. Dekel, *astro-ph/0105470* (2001).
- [3] R. M. Cutri and M. F. Skrutski, *Bull. Am. Astron. Soc.* 30, 1374 (1998).
- [4] D. A. Dale, R. Giovanelli, M. P. Haynes, et al., *Astrophys. J.* 510, L11 (1999).
- [5] A. Dekel, A. Elder, T. Kolatt, et al., *Astrophys. J.* 522, 1 (1999).
- [6] S. M. Faber and R. E. Jackson, *Astrophys. J.* 204, 668 (1976).
- [7] W. K. Huchtmeier, I. D. Karachentsev, V. E. Karachentseva, et al., *Astron. Astrophys.* 435, 459 (2005).
- [8] M. J. Hudson, *astro-ph 0311072* (2003).
- [9] M. J. Hudson, R. J. Smith, J. R. Lucey, et al., *Mon. Not. R. Astron. Soc.* 352, 61 (2004).
- [10] T. H. Jarrett, *Publ. Astron. Soc. Pac.* 112, 1008 (2000).
- [11] T. H. Jarrett, T. Chester, R. Cutri, et al., *Astron. J.* 119, 2498 (2000).
- [12] I. D. Karachentsev, V. E. Karachentseva, Yu. N. Kudrya, et al., *Bull. Spec. Astrophys. Obs.* 47, 5 (1999).
- [13] I. D. Karachentsev, V. E. Karachentseva, Yu. N. Kudrya, et al., *Astron. Zh.* 77, 175 (2000) [*Astron. Rep.* 44, 150 (2000)].
- [14] I. D. Karachentsev, V. E. Karachentseva, and S. L. Parnovskii, *Astron. Nachr.* 314, 97 (1993).
- [15] I. D. Karachentsev and D. I. Makarov, *Astron. J.* 111, 794 (1996).
- [16] I. D. Karachentsev, S. N. Mitronova, V. E. Karachentseva, et al., *Astron. Astrophys.* 396, 431 (2002).
- [17] A. Kogut, C. Lineweaver, G. F. Smoot, et al., *Astrophys. J.* 419, 1 (1993).

- [18] Yu. N. Kudrya, V. E. Karachentseva, I. D. Karachentsev, et al., *Astron. Astrophys.* 407, 889 (2003).
- [19] T. R. Lauer and M. Postman, *Astrophys. J.* 425, 418 (1994).
- [20] S. N. Mitronova, I. D. Karachentsev, V. E. Karachentseva, et al.), *Bull. Spec. Astrophys. Observ.* 57, 5 (2004).
- [21] S. N. Mitronova, W. K. Huchtmeier, I. D. Karachentsev, et al., *Pis'ma Astron. Zh.* 31, 563 (2005) [*Astron. Lett.* 31, 501 (2005)].
- [22] P. J. E. Peebles, *The Large-Scale Structure of the Universe* (Princeton Univ. Press, Princeton, 1980; Mir, Moscow, 1983).
- [23] D. J. Radburn-Smith, J. R. Lucey, and M.J. Hudson, *astro-ph/0409551* (2004).
- [24] A. G. Riess, M. Davis, J. Baker, et al., *Astrophys. J.* 488, L1 (1997).
- [25] W. Saunders, W.J. Sutherland, S. J. Maddox, et al., *Mon. Not. R. Astron. Soc.* 317, 55 (2000).
- [26] J. L. Tonry, J. P. Blakeslee, E. A. Ajhar, et al., *Astrophys. J.* 530, 625 (2000).
- [27] R. B. Tully and J. P. Fisher, *Astron. Astrophys.* 54, 661 (1977).
- [28] J. A. Willick, *Astrophys. J.* 522, 647 (1999).
- [29] J. A. Willick, *astro-ph/0003232* (2000).
- [30] S. Zaroubi, *astro-ph/0206052* (2002).